Diastereomeric Selective Effects of Double-Stranded Peptides Conjugated with –Phe–Phe– Residue for Growth Inhibition and Permeability of Ca^{2+} on A431, *src*^{ts}NRK, and A549 Cells Proliferation

Shigeki KOBAYASHI,* Hidetaka WAKAMATSU, Nahomi ATUCHI, Rie MIYAJIMA, Ayumi KAWADA, and Mayuko HATTORI

Department of Analytical Chemistry of Medicines, Showa Pharmaceutical University; 3–3165 Higashi-Tamagawagakuen, Machida, Tokyo 194–8543, Japan. Received April 17, 2006; accepted October 30, 2006

Our aim in this study is to elucidate the correlations between inhibition and chirality, especially, diastereomer, against cell proliferation of double-stranded peptides. In previous studies, we reported on the design, synthesis, and chemical properties on a series of novel double-stranded peptides, (y-AA–x-AA)$_2$–spacer(S) (AA=amino acid, S=spacer, symbols x and y represent L- or D-forms, and (y-, x-) as represent of the symbol) conjugated with –y-AA–x-AA– and –z-AA–y-AA–x-AA– sequences to a spacer of carbon number *n*. The inhibition of A431 and *src*^{ts}NRK cells growth by four diastereomers of the N^1,N^{12}-bis(y-Phe–x-Phe)dodecanediamines (*n*=12) increased in the following order: (L-, L-)<(D-, D-)<(L-, D-)<(D-, L-). A similar trend was seen in the order for the activity of (y-AA–x-AA)$_2$–spacer(S) with a spacer of carbon number *n*=2, 3, 4, 5, 6, and 12 against the cell growth inhibition. To understand the mechanism of diasteromer selective cell growth inhibition, the correlations between chirality and cell growth inhibition were investigated from the measurement of the changes in cytosolic Ca^{2+} concentration (=$[Ca^{2+}]_c$) of A431 cells. Although less active N^1,N^{12}-bis(L-Phe–L-Phe)dodecanediamine increases cytosolic $[Ca^{2+}]_c$, more active diasteromers, N^1,N^{12}-bis(L-Phe–D-Phe)dodecanediamine and N^1,N^{12}-bis(D-Phe–L-Phe)dodecanediamine, decrease cytosolic $[Ca^{2+}]_c$ in A431 cell. This study provides diastereomeric effected new insights—this controls the polarity of double-stranded peptides—into the control of tumor cell proliferation and design of the uptake by penetration through the cell membrane of drugs.

Key words double-stranded peptide; diastereomer; chirality; cell growth inhibition; tumor cell; Ca^{2+} concentration

In a previously published study, we designed and synthesized parallel double-stranded peptides (**1**), bis(z-Phe–y-Phe–x-Val)$_2$–spacer(S) and bis(y-Phe–x-Phe)$_2$–spacer(S) (symbols x, y and z=L- or D-configurations, AA=amino acid, S=spacer, and Phe=phenylalanine), conjugated with two –Val–Phe–Phe– and –Phe–Phe– peptide residues, respectively, to a polyamine spacer.[1,2] The –Val–Phe–Phe– and –Phe–Phe– sequences are π-electron rich and in hydrophobic sequence, and the appearance rate is low in the natural proteins. For example, the appearance rates of the –Phe–Phe– and –Val–Phe–Phe– sequences in a human progesterone receptor form B (hPR; 933AA (AA=amino acid)[3]) were 0%. However, these sequences are also contained in the positions from 21st to 23rd in β-amyloid (Aβ) peptide in Alzheimer's disease.[4,5] Thus, the Phe–Phe sequence as a hydrophobic amino acid may be playing an important role in cell viability, but the biological role and effects are not known at all. To elucidate the chemical and biological functions, we are very interested in designing functional double-stranded peptides improving on cell growth inhibition, penetration, and viability by conjugation of Phe and Phe–Phe. The introduction of π-electron rich and a hydrophobic side chain in the double-stranded peptides can have a role of molecular inclusion and recognition by interaction between the double-stranded peptide and the target.[1] In addition, four optical isomers, (L-, L-), (D-, L-), (L-, D-), and (D-, D-), to bis(y-Phe–x-Phe)$_2$–spacer(S) are possible in the synthesis and we synthesized them.

From a pharmacological standpoint, we are interested in what difference four optical isomers, enantiomer and diastereomer, have on the viability of living cells. Especially, the anti-proliferative effects on tumor cells of the diastereomers are poorly understood when compared with that of the enantiomer. Here, our aim in this study is to understand better the structure–activity relationships between cell anti-proliferative effects and four optical isomers of the classes of bis(y-Phe–x-Phe)$_2$–spacer(S). We found that the bis(y-Phe–x-Phe)$_2$–spacer(S)s are very valuable for investigating the anti-proliferative effect of tumor cells since the evidence for the configurational pattern of the compound-target cell interaction on cell death is lacking.

In stimulation of N^1,N^{12}-bis(y-Phe–x-Phe)dodecanediamine (**18a**—**d**) to *src*^{ts}NRK cells,[6,7] for instance, we first found that the growth inhibitory decreases in the following order: bis(L-Phe–D-Phe)– (**18c**)>bis(D-Phe–L-Phe)– (**18b**)> bis(D-Phe–D-Phe)– (**18d**)≫N^1,N^{12}-bis(L-Phe–L-Phe)dodecanediamine (**18a**). Similar trends were also observed for other cells, such the A431 and A549 cells.[8,9] These results indicate that the diastereomers, (D-, L-) and (L-, D-) are more potent than the (L-, L-) configuration. The death of *src*^{ts}NRK and A431 cells is controlled in the chilarity of **18a**—**d**. The geometric control by the diastereomers of the cell growth inhibition (IC_{50}) may present good advantages for the uptake of the drug. Because the double-stranded peptides interact with the cell membrane and may play an important role in the transportation of polyamines,[10] Na^+, and Ca^{2+} ions into cells. In order to understand the role of the chilarity of bis(y-Phe–x-Phe)$_2$–spacer(S) on cell growth inhibition, the change in cytosolic Ca^{2+} concentration ($[Ca^{2+}]_c$) was measured by fluorometry using Fura-2.[11] It was found that the change of the cell membrane's permeability of Ca^{2+} by treatment of bis(y-Phe–x-Phe)$_2$–spacer(S) is correlated to the growth inhibition of the diastereomers on the cell death. The exact mechanisms for the diastereomeric difference of intracellular $[Ca^{2+}]$ concentration suggest that bis(y-Phe–x-Phe)$_2$–spacer(S)s form

* To whom correspondence should be addressed. e-mail: kobayasi@ac.shoyaku.ac.jp

the double-stranded peptide–membrane complexes on the cell membrane or affect the specific receptor implicated in the cell growth inhibition.

The relationship between IC_{50} and changes in cytosolic $[Ca^{2+}]_c$ for the cell growth inhibition by treatment of the diastereomers may be explained by the polarity of N^1,N^{12}-bis(y-Phe–x-Phe)dodecanediamines such as **18a** and **18b**. Finally, our study provides new first insights concerning the structurally diverse relationship between diasteromeric effects and cell proliferation. In addition, we give the correlation on the cell growth inhibition between the polarity of the diastereomers and changes in cytosolic $[Ca^{2+}]_c$. Such a diastereomerical chemotherapy using diastereomeric double-stranded peptides or other related analogs may become possible in the future in the field of cancer chemotherapy.

Experimental

General Methods Melting points were determined on a Yanako (MP-21) apparatus and are uncorrected. The peptides were detected on TLC plates using iodine vapor or UV absorption. Silica gel column chromatography was performed using Silica gel 60 N (100 mesh, neutral, Kanto Chemical, Tokyo). The solvent systems were as follows: A, $CHCl_3$–MeOH (20 : 1) and B, $CHCl_3$–MeOH (10 : 1). ^{1}H- and ^{13}C-NMR spectra were obtained using a JEOL α-500 NMR spectrometer and NMR samples were dissolved in $DMSO_{d6}/CDCl_3$ (volume: 0.5 ml/0.2 ml) with TMS as an internal reference. FAB mass spectral data were obtained on a JEOL JMS-HX110 spectrometer, and relevant data was tabulated as *m*/*z*. Elemental analyses were performed by the Laboratory Center of Elemental Analysis, University of Ehime (Matuyama, Japan).[2)]

Drugs and Chemicals Boc–L-PheOH and Boc–D-PheOH were from Peptide Lab. Dulbecco's modified Eagle's medium (DMEM) and fetal bovine serum (FBS) were obtained from Peptide Dainippon Co. (Tokyo). The cellular toxicity kit (WST-1 or Kit-8) and fura2-AM were from Dojindo Laboratories (Tokyo). All other chemicals were purchased from Sigma-Aldlich Japan K.K. (Tokyo) and Wako Pure Chemical Ind., Ltd. (Osaka, Japan) unless otherwise stated.

Synthesis of Double-Stranded Peptides (1) The double-stranded peptides, **13a**—**d**, **15a**, **b**, **16a**, **b**, **17a**—**d**, and **18a**—**d** used in this study were prepared according to the procedures described in our previously published methods.[1,2)]

***N*^{1},*N*^{3}-bis(L-Phe–L-Phe)propanediamine (14a)** Compound N^1,N^3-bis(*t*-butoxycarbonyl L-Phe–L-Phe)propanediamine (**8a**) was prepared according to the procedures described in our methods,[2)] and was obtained in 81.0% yield, and the crude product (2.3 g) was purified by column chromatography on silica gel (41 g) eluted with $CHCl_3$ and 3% MeOH–$CHCl_3$ (stepwise elution); mp 200—202 °C (from MeOH); *Rf* (A): 0.61; HR-FAB-MS (nitrobenzyl alcohol) *m*/*z* (MH^+) Calcd for $C_{49}H_{63}N_6O_8$: 863.4707. Found: 863.4708. To a solution of **8a** (2.0 g, 2.39 mmol) was added TFA (15 ml). The mixture was stirred for 1 h in an ice bath. After a 5% $NaHCO_3$ and 1 M NaOH workup, the crude solid **14a** was collected, washed with water, and dried *in vacuo*. Compound **14a** was purified by silica gel column chromatography eluted with $CHCl_3$ and 3% MeOH/$CHCl_3$ (stepwise elution); mp 105—106 °C (from MeCN/MeOH); *Rf* (B): 0.53; ^{1}H-NMR ($CDCl_3/DMSO_{d6}$=0.5/0.2 ml) δ 1.42–1.46 (m, 2H, –(CH_2)–), 2.55 (dd, J=8.85, 13.74 Hz, 1H, βH^1 in Phe^1), 2.92—3.04 (m, 5H, βH^2 in Phe^2×2, βH^1 in Phe^1 and –CH_2NHCO–), 3.59 (dd J=4.57, 8.85 Hz, 1H, αH^2 in Phe^2), 4.57 (ddd, J=7.63, 8.24, 13.73 Hz, 1H, αH^1 in Phe^1), 7.12—7.18 (m, 5H, Phe), 7.19—7.28 (m, 5H, Phe), 7.71 (t, J=6.10 Hz, 1H, –NH^aCO–), and 8.06 (d, J=8.24 Hz, 1H, –NH^bCO–); ^{13}C-NMR ($CDCl_3/DMSO_{d6}$= 0.5/0.2 ml) ppm 28.74, 35.41, 37.94, 40.03, 53.88, 55.93, 126.45, 126.50, 128.12, 128.33, 129.19, 129.27, 137.06, 137.50, 171.03, and 173.27; HR-FAB-MS (nitrobenzyl alcohol) *m*/*z* (MH^+) Calcd for $C_{39}H_{47}N_6O_4$: 663.3654. Found: 663.3668.

***N*^{1},*N*^{3}-bis(D-Phe–L-Phe)propanediamine (14b)** mp 208—210 °C (from MeCN/MeOH); *Rf* (B): 0.13; HR-FAB-MS (nitrobenzyl alcohol) *m*/*z* (MH^+) Calcd for $C_{39}H_{47}N_6O_4$: 663.3654. Found: 663.3684.

Computational Chemistry The search for low-energy and optimized conformations of double-stranded peptide analogs were done using SPARTAN'04 and SPARTAN5 programs[12)] running on a personal computer and Compaq DS10 workstation, respectively.

Cell Line and Culture The A431 and A549 cell lines were obtained from The RIKAGAKU institute (Tsukuba, Japan), and the *src*^{ts}NRK cell line was donated by Prof. Kayoko Tsuchiya (Showa Pharmaceutical University, Tokyo). Stock cells were cultures in DMEM containing 0.37% sodium bicarbonate, 100 units/ml of penicillin G, and 100 μg/ml streptomycin sulfonate supplemented with 10% heat inactivated FBS, in a water-jacketed 5% CO_2 incubator; the medium was exchanged every 3 d. For the experiments, the cells were seeded at a density of 5.0×10^5 cells/ml in tissue culture flasks (25 cm^2/ml) in 10% FBS/DMEM.

Cell Growth Inhibition Assay To measure the effect on the cell proliferation by various concentrations of the double-stranded peptides, A431, A549, and *src*^{ts}NRK cells ($1.0—2.0\times10^5$ cells/ml) were reseeded in flat bottom 96-well micro-assay plates (180 μl/well) and incubated for 24 h at 33 °C (or 39 °C). The double-stranded peptides diluted in dimethylsulufoxide (DMSO) (5V/V%) were then added to the 96-well micro-assay plates and incubated for 4 d at 33 °C (or 39 °C) in a humidified atmosphere containing 5% CO_2 in the air. The effects on cell growth were determined by cell counting; cell viability was measured as the reduction (10 μl) WST-1 (or Kit-8) (modified 3-(4,5-dimethyl-2-thiazolyl)-2,5-diphenyl-2*H*-tetrazolium bromide (MTT) assay) and the results were confirmed by scanning with a BIO-RAD Model 680 microplate reader (BIO-RAD Japan, Tokyo) using 450 nm as the measurement filter and 630 nm as the reference filter. The value (IC_{50}; the concentration for a 50% inhibition of cell growth) of the cell growth inhibition computed by a log(dose)-response curve obtained by the modified MTT assay.

StatView J-4.5 was used on the statistical analysis of the data. The data is given in mean values and standard error of mean (S.E.M.) of three experiments or two independent determinations at $<\pm5\%$ of the absolute error. Comparisons between means of (L-, L-) and (D-, L-) forms were made using the *t*-test assuming significance at $p<0.05$.

Measurement of Cytosolic Free Ca^{2+} Concentration To load fura2-AM to A431 cells, the cells (6×10^6 cells/mI) were incubated in the culture medium containing fura2-AM (1 mM) for 0.5 h at 37 °C. Then the cells loaded fura2-AM were washed two times by Ca^{2+} free Hepes buffer (140 mM NaCl, 5 mM KCl, 1.2 mM $MgCl_2$, 1.0 mM glucose, 0.3% BSA, and 20 mM Hepes) saline in order to remove and to be hydrolysis excess fura2-AM, and stand for 15 min at room temperature. The cells were washed by centrifugation and suspended in the Ca^{2+} free Hepes buffered saline. After the cell counting, the cells were used for fluorometry. The fura-2 was excited at wavelengths of 340 and 380 nm. The fluorescence was measured at 500 nm and corrected for autofluorescence.

Here, cytosolic free $[Ca^{2+}]_c$ was determined from the ratio (R) of the fluorescence signals at both wavelengths. Where, $[Ca^{2+}]_c=K_d[(R-R_{min})/(R_{max}-R)](F_{380max}/F_{380min})$ and K_d is the dissociation constant, R_{min} is the minimum ratio (F_{340}/F_{380}) in zero Ca^{2+}, and R_{max} is the maximum ratio (F_{340}/F_{380}) at saturated Ca^{2+}. Calibrations used values of $F_{380max}/F_{380min}=1.2$ and $K_d=224$ nmol/l.[13)] The fluorescent signals were detected by an RF-5000 fluorospectrophotometer (Shimadzu, Kyoto, Japan). Calibration and calculation of the free $[Ca^{2+}]$ concentration from the fluorescence ratio were achieved according to detailed methods described elsewhere.[14)]

Results and Discussion

Structure and Chemistry The double-stranded peptides used in this study were synthesized in a good yield by using procedures described in our previous paper.[1,2)] The pathway of the synthesis of the target compounds was shown in Fig. 1.

To search the conformations of the double-stranded peptides, we used the NOESY technique and computational chemistry.[15,16)] The later method computed the most stable structures from the conformation searched by the MONTE-CALRO method using MMFF (molecular mechanics), and the structure was minimized by a *ab initio* Hartree–Fock (HF) calculation using a 6-31G* basis set. NMR data show that the dihedral angle of ∠–CO–CH^1–NH^b–CO–, ϕ, in N^1,N^6-bis(L-Phe–L-Phe)hexanediamine (**17a**) is about $-87°$ based on the $^3J_{NHa,CHa}$=8.55 Hz ($d_{\alpha N}$). The value indicates β-sheet-like conformation since the $^3J_{NHa,CHa}$ value is the acceptable range for β-sheet structure (7.0—10.0 Hz).[17,18)] The dihedral angle of ∠–CH_2–CH_2–NH^a–CO–, ω, based on coupling constant ($J_{NHa,CH}$=5.5 Hz) between NH^aCO (δ 7.47)

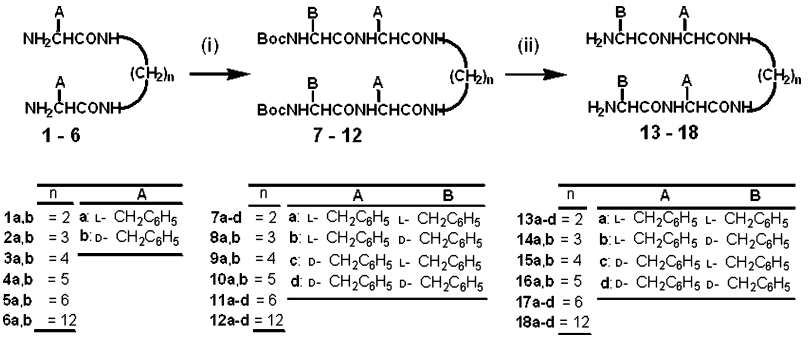

Fig. 1. Pathway of the Synthesis of Parallel Double-Stranded Peptide Conjugated Amino Acids

Key; (i) CDI, BocAAOH (AA=amino acid residue), in dry $CHCl_3$. (ii) (1) TFA at 4 °C, (2) 5% $NaHCO_3$, 1 M NaOH.

and $-(CH_2)-$ of the spacer in **17a** is about 90°. The dihedral angle, ∠–NH^a–CO–CH–NH^b–, φ, was here free and the angle was computed by optimization with the HF method using 6-31G* basis set. Figure 2 shows the optimized conformations of **14a**, **b**, **15a**, **b**, **17a**, **b**, and **18a**, **b**. The intrastranded NOE connectivities between aromatic protons of Phe (at δ 6.72 and 6.96) and $-CH_2-$ protons of the spacer in **17a** indicate that a S symbolic turn is required for the formation of the β-sheet-like nucleation, as shown in Fig. 2C.

Our aim is understanding of the structure of N^1,N^6-bis(D-Phe–L-Phe)hexanediamine (**17b**) containing D-Phe residue as compared with that of **17a**. Computed results show that the total energy (E_{total}=−2247.02141 au) of **17a** is larger than that (E_{total}=−2247.01718 au) of **17b** in the gas phase. Compound **17a** and **18a** is more stable than **17b** and **18b** by 2.7 and 4.6 kcal/mol in total energy at HF/6-31G* level. However, compounds **14b** and **15b**, inversely, are more stable than **14a** and **15a**, as summarized in Table 1. This stabilization may be due to the carbon number of the spacer. This reason is expected because of hydrophobic interaction and hydrogen bonding in **14**, **15**, **17**, and **18**. In addition, the solvation energy of **14a** and **15a** are −32.33 and −20.56 kcal/mol. The values are larger than the values of −3.69 and −3.50 kcal/mol of their diastereomers,**14b** and **15b**, respectively. They provide good soluble structure in water.

There is a good hydrogen bond in **17a** and **15a**, as indicated by the C=O···H_2NCH– distance of 0.215 nm (a) and 0.210 nm (b) and C=O···H_2NCH– distance of 0.209 nm (b) and 0.199 nm (a), respectively. The data of the hydrogen bond is shown in Table 1 and Fig. 2. In addition, the magnitude of the polarity is related to the charge distribution in the molecules. The electric dipole moment is one of the measures. In order to obtain the effect on the electric dipole moment of D-Phe residue, we used *ab initio* HF/6-31G* calculations for the target double-stranded peptides. The electric dipole moments of the diastereomers **14b**, **15b**, **17b**, and **18b** are larger values than all L-forms **14a**, **15a**, **17a**, and **18a**. It was found that the diastereomers containing D-Phe residue possess large polarity (Table 1).

The calculation data by HF/6-31G* level show that the dihedral angle ∠–CO–CH^1–NH^b–CO– (ϕ) in **17a** is about −84.1° and is a similar with the value obtained by the NMR data. We previously described that the date is the acceptable range for β-sheet-like structure. Therefore, it is suggested that the graphical date of **17a** shown in Fig. 2C is certain of the conformation in the solution. The date of *ab initio* HF/6-31G* calculations for **14a**—**b**, **15a**—**b**, and **18a**—**b** also show similar results with the experimental date.

Growth Inhibition of A431 and *src*^{ts}NRK Cells Table 2, Figs. 3 and 4 show IC_{50} values of A431, A549, and *src*^{ts}NRK cells cultured for 4 d with the double-stranded peptides **13a**—**d**, **17a**—**d**, and **18a**—**d**. The IC_{50} is defined as the concentration (mol/l or M) of **13a**—**d**, **17a**—**d**, and **18a**—**d** which reduces cell viability by 50%. Against A431 cells, N^1,N^2-bis(L-Phe–L-Phe)ethanediamine (**13a**) was effective at 406 μM, while the enantiomer, N^1,N^2-bis(D-Phe–L-Phe)-ethanediamine (**13b**), was more potent (32.8 μM) than **13a**. N^1,N^2-Bis(L-Phe–D-Phe)ethanediamine (**13c**) also affected cell proliferation, and its effect was significant at 32 μM. Furthermore, the IC_{50} value of **17a** was significant at 101 μM. Similarly, the activity of the diastereomer, N^1,N^6-bis(L-Phe–D-Phe)hexanediamine (**17c**) (30 μM), also was greater than that of **17a**. These results are shown in Figs. 3A and C.

To understand more the chilarity effect of the L- and D-configuration, the inhibition of cell growth was evaluated on treatment with several synthesized double-stranded peptide analogs **18a**—**d**. For example, the compounds **18a** and **18c** blocked temperature-sensitive *src*^{ts}NRK[7] cell growth at 19.6 μM and 2.4 μM, respectively. Furthermore, **13a** and **13c** inhibited *src*^{ts}NRK cell proliferation with an IC_{50} value of 387 μM and 53 μM, respectively, as shown in Fig. 3B. Although the diastereomers **13b**, **c** and **18b**, **c** obviously, are more active than **13a** and **18a**, similar trends were observed in compounds **13** and **18**, as shown in Fig. 4B. The activity of compound **18a** is also weakest and, evidently, **18b**, **18c** and **18d** conjugated with D-Phe exhibited a potent effect on A549 cells, as shown in Fig. 4A. In addition, the diastereomer **18b** had a more potent inhibitory effect on transformed at 33 °C than normal *src*^{ts}NRK cells at 39 °C. Therefore, compound **18b** prefers to inhibit the transformed morphology rather than the normal morphology.

The IC_{50} values were inhibitory to cell growth at 10^{-4}—10^{-6} mol/l. The (L-, L-) (or (D-, D-)) configuration in **18a** is less active, while the chirality of (D-, L-) and (L-, D-) increases the inhibitory effect on cell growth. The inhibitory effect on *src*^{ts}NRK, A549, and A431 cell growth increases in the following order: (L-, L-)≪(D-, D-)<(D-, L-)~(L-, D-). It suggests that the diastereomers (D-, L-) and (L-, D-) play an important role in the cell death.

Effect of Carbon Number of Spacer on A431 Cells Proliferation To investigate the relationship between the carbon number of the spacer, chirality, and antiproliferative ef-

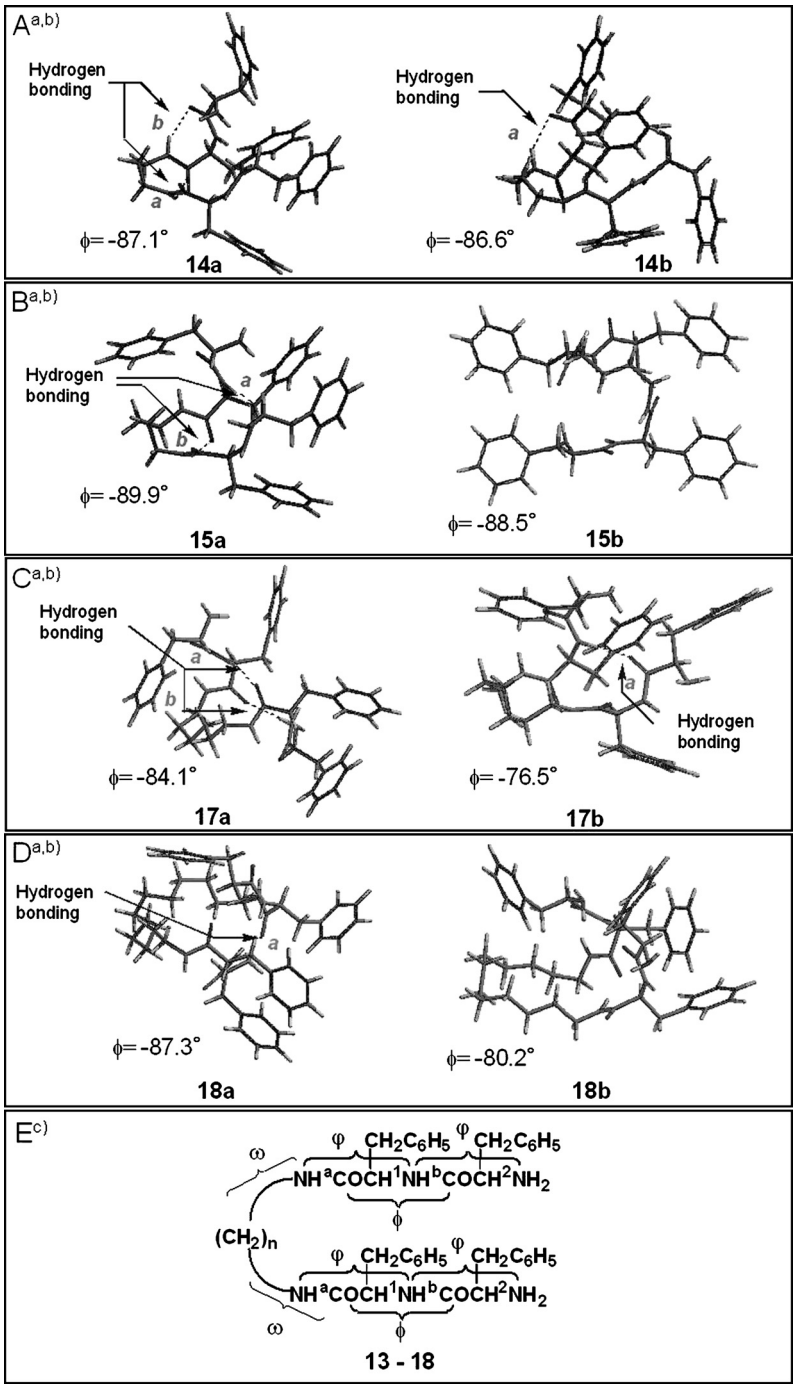

Fig. 2. Tube Showing (A—D) of Molecular Structures for Optimized Double-Stranded Peptides **14a**, **b**, **15a**, **b**, **17a**, **b**, and **18a**, **b**

a) At *ab initio* HF/6-31G* level. *b*) *Ab initio* HF/6-31G* level conformational model of diastereomers **14a**, **b** (A), **15a**, **b** (B), **17a**, **b** (C), and **18a**, **b** (D). The ∠–CO–CH^1–NH^b–CO– dihedral angle is φ (°). *c*) Several dihedral angles, ϕ, φ, and ω, in double-stranded peptides (E). The computed values were consistent with experimental values.

fect on A431 cells, the IC_{50} values of double-stranded peptides **13a**—**18a** and **13b**—**18b** were obtained using a similar method. The results are shown in Fig. 5. Figure 5 shows that N^1,N^4-bis(L-Phe–L-Phe)butanediamine (**15a**) (IC_{50}>1230 μM) had less antiproliferative activity toward the compounds tested. For example, compound **16b** affects A431 cell growth inhibition more actively than **16a** since the IC_{50} values are 56.5 μM and 904 μM, respectively. We found, obviously, that the diastereomers (D-, L-) **13b**—**18b** are more potent than the (L-, L-) forms **13a**—**18a**, and the antiproliferative activity of the (D-, L-) forms increased in the following order; **15b** C(4)<**14b** C(3)<**16b** C(5)<**13b** C(2)<**17b** C(6)<**18b** C(12) (number of carbon). On the inhibitory activity, the diasteromeric selective effects were observed for double-stranded peptides with several carbons (n=2, 3, 4, 5, 6, 12). Generally, the inhibitory effect of the diastereomers against A431 cells is more pronounced than that of the enantiomers; (L-, L-)<(D-, L-). The effect has no relationship on the carbon number of the spacer. For example, although the cell growth inhibition of N^1,N^2-bis(y-Phe–x-Phe)ethanediamines **13a**

Table 1. Comparison of Total Energy Differences and Dipole Moment of Optimized Double-Stranded Peptides

Compound	Carbon number of spacer	Configuration (y-, x-)	Total energy[a] (au)	ΔE_{total}[b] (kcal/mol)	Dipole moment[a] (Debye)	Hydrogen bonding[c] (number)	Position[d]	Length of hydrogen bonding (nm)
14a	3	(L-, L-)	−2129.91110	0	2.40	2	a	0.198
							b	0.206
14b	3	(D-, L-)	−2129.91316	−1.3	3.02	1	a	0.208
15a	4	(L-, L-)	−2168.94865	0	1.45	2	a	0.199
							b	0.209
15b	4	(D-, L-)	−2168.95971	−6.9	1.36	0	—	—
17a	6	(L-, L-)	−2247.02141	0	1.82	2	a	0.210
							b	0.215
17b	6	(D-, L-)	−2247.01718	+2.7	2.17	1	a	0.209
18a	12	(L-, L-)	−2481.23005	0	0.54	1	a	0.220
18b	12	(D-, L-)	−2481.22278	+4.6	2.61	0	—	—

a) At HF/6-31G* level. *b*) For example, ΔE_{total} represents the gap of total energy (E) between E_{15b} and E_{15a}; $\Delta E_{total}=E_{15b}-E_{15a}$. *c*) Amount of intramolecular hydrogen bonding, C=O···HN. *d*) The a and b represent positions of the hydrogen bonding as shown in Fig. 2.

Table 2. Configuration Effects of Double-Stranded Peptides, **18a**—**18d**, on the Changes in Cytosolic Ca^{2+} Concentration of A431 Cells

Compound	Configuration	$[Ca^{2+}]_c$[a,b] (nM) Compounds, **18a**—**d**			IC_{50}[f] (μM)
		FBS	FBS[c]	without FBS[d]	
Control	—	+21.6±6[e,f]	+21.6±6[e,f]	—	
18a	(L-, L-)	—	+91.3	+170.9	49.5±1.55[g]
18b	(L-, D-)	—	+24.6	+46.0	6.6
18c	(D-, L-)	—	+25.1	+29.9	6.7
18d	(D-, D-)	—	+21.1	+36.7	6.8

a) Fura2-AM loaded A431 cells were preincubated with 1 μM (final concentration) of **18a**, **b**, **c**, and **d**, respectively, as described in Methods. *b*) Cytosolic free Ca^{2+} concentration represents the mean of two determinations. *c*) After FBS was treated and the baseline was stabilized (after about 3—4 min), the compounds **18a**, **b**, **c**, and **d** were treated. *d*) After the baseline was stabilized, the compounds **18a**, **b**, **c**, and **d** were treated. *e*) Cytosolic free Ca^{2+} concentration was measured after FBS was treated and the baseline was stabilized (control). *f*) The IC_{50} values represent the mean of two determinations at <±5% of the absolute error. *g*) The IC_{50} values represent the mean±S.E.M. of the three independent determinations.

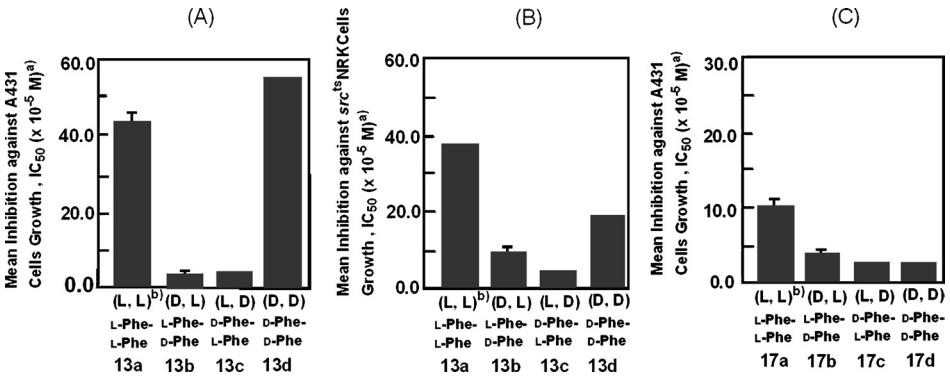

Fig. 3. Diastereomeric Effects on Growth of A431 and *src*[ts]NRK Cells by Treatment with Double-Stranded Peptides **13a**—**d** and **17a**—**d**

a) A431 and *src*[ts]NRK cells were treated with or without double-stranded peptides **13a**—**d** (A), **17a**—**d** (C), and **13a**—**d** (B) for 4 d at 37 °C, respectively, and then IC_{50} values were determined as described under Methods. Each of the bars are the mean of two independent determinations at <±5% of the absolute error. The vertical small bar is the error bar as mean±S.E.M. of IC_{50} values in mol/l of three independent determinations. *b*) A parenthesis (y, x) expresses configurations of the compounds **13a**—**d** and **17a**—**d**.

(IC_{50}=426 μM) and **b** (34.3 μM) conjugated with a short length spacer, –CH_2–CH_2–, is less active than that of compounds **18a** (49.5 μM) and **b** (6.6 μM), the antiproliferative activity is more active than that of compounds **15a** (>1230 μM) and **b** (639 μM).

The length of the spacer also conferred specific inhibitory effects. For instance, the compound **15a**—carbon number of the spacer is four—is more inactive than the corresponding double-stranded peptides (Fig. 5). The inhibitory potency in **13a**—**18a** series increased in the following order: C(4)<C(5)<C(3)<C(2)<C(6)<C(12). We found, furthermore, that the diastereomers, **13b**—**18b** series, have more activity than enantiomers, **13a**—**18a**, on A431 cell viability. Why is the spacer with four carbons the most inactive? The spacer of **15a** is putrescine (n=4) which is classified as a biogenic polyamine.[19] It is reported that tumors increase the rate of putrescine uptake.[20] Therefore, the compound **15a** is recognized by putrescine receptors on the cell membrane, and it may be much less potent than **18a** and **18b**, *etc*.

Measurements of Cytosolic Ca^{2+} Concentration Using

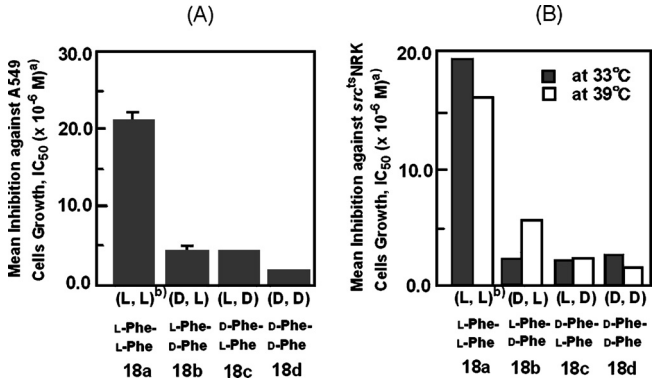

Fig. 4. Diastereomeric Effects on Growth Inhibition of A549 and *src*^{ts}NRK Cells by Treatment with Double-Stranded Peptides **18a**—**d**

a) A549 cells were treated with or without double-stranded peptides **18a**—**d** for 4 d at 37 °C. *Src*^{ts}NRK cells were treated with or without double-stranded peptides **18a**—**d** for 4 d at 33 °C and 39 °C, respectively. IC_{50} values were determined as described under Methods. Each of the bars are the mean of two independent determinations at $<\pm5\%$ of the absolute error. The vertical small bar is the error bar as mean±S.E.M. of IC_{50} values in mol/l of three independent determinations. *b*) A parenthesis (y, x) expresses configurations of the compounds **18a**—**d**.

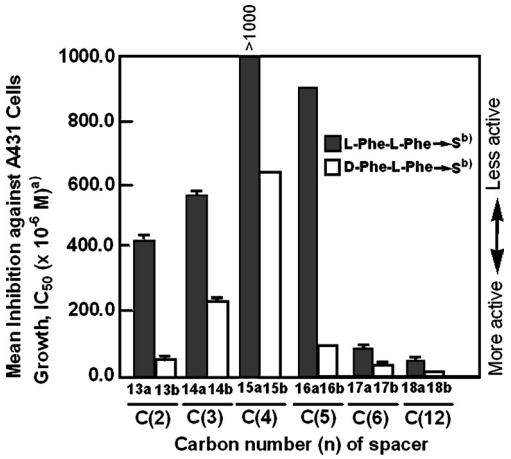

Fig. 5. Relationship between Chirality, Carbon Number, and Inhibitory Effect of Double-Stranded Peptides **13**, **14**, **15**, **16**, **17**, and **18** on A431 Cell Proliferation

a) A431 cells were treated with or without double-stranded peptides **13a**, **b**, **14a**, **b**, **15a**, **b**, **16a**, **b**, **17a**, **b**, and **18a**, **b** for 4 d at 37 °C, then IC_{50} values were determined as described under Methods. Each of the bars are the mean of two independent determinations at $<\pm5\%$ of the absolute error. The vertical small bar is the error bar as mean±S.E.M. of IC_{50} values in mol/l of three independent determination. The C(*n*) number is the amount of carbons in the spacer in double-stranded peptides. *b*) A symbol S expresses a spacer.

Fura2-AM We are interested in the correlation for cell death between the diastereomeric effects and change of cytosolic free Ca^{2+} concentration ($[Ca^{2+}]_c$) by **18a** and **18b** in A431 cells. In order to understand whether the diastereomeric effects of bis(y-Phe–x-Phe)$_2$–spacer(S) on the cell growth inhibition are correlated with the changes in $[Ca^{2+}]_c$, the changes in the $[Ca^{2+}]_c$ of A431 cells stimulated with **18a**—**d** was measured by fluorometry with Ca^{2+}-sensitive fluorescent indicator (fura2-AM) according to the methods described in the experimental section.

Figure 6 shows the changing of the time-dependent ratio of F_{340}/F_{380} ($=R$) for A431 cells treated with diasteromer **18b**. The $[Ca^{2+}]_c$ of A431 cells loaded fura2-AM which were treated with 1 μM (final concentration) of **18b** and **18c** was about 21—25 nM, respectively. However, the treatment of

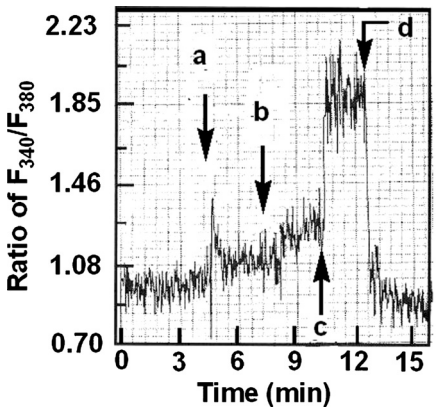

Fig. 6. Measurement of Changes of Cytosolic $[Ca^{2+}]_c$ concentration in A431 Cells Loaded with Fura2-AM by Treatment of Double-Stranded Peptides **18a**—**d**

A431 cells were loaded with Fura2-AM and incubated in the standard medium supplemented with calcium-free HEPES saline. The A431 cells were added FBS (a), and 4 min later the cells were added with subsequent additions of 16.5 μl of double-stranded peptides **18b** (1.0 μM final concentration) (b). After 4—5 min, the cells were exposed to the Triton X100 (c), and 1.5 mM EGTA were added (d). In each panel one trace, typical of the seven collected, is shown.

1 μM (final concentration) **18a** gave a pronounced increase in mean cytosolic $[Ca^{2+}]_c$ of 91 nM. When A431 cells were not treated with FBS, the addition of **18a** presented a striking increased in mean $[Ca^{2+}]_c$ of 171 nM. The results are summarized in Table 2.The rapid increases of $[Ca^{2+}]_c$ have these two reasons; first, inflow of extracellular origin $[Ca^{2+}]_e$, second, Ca^{2+} releases from cytosolic microsome and mitochondria. Our results indicate that after A431 cells treated with bis(L-Phe–L-Phe)$_2$–spacer(S)s **18a** or **18b**, **18a** or **18b** uptake in the membrane and cytosol of A431 cells. Indeed, fluorescence microscopic images of A431 cells by the double-stranded peptide conjugated fluorescence dansyl group show the double-stranded peptide uptakes in the cell membrane and cytosol of A431 cells.[2)]

As the mean $[Ca^{2+}]_c$ of A431 cells used was 70 nM, the mean change of 21—25 nM indicates that compounds **18b**, **18c**, and **18d** containing D-Phe accelerated the outflow of Ca^{2+} from innercellular to outer cellular.

***Rf* Values and Proposed Double-Stranded Peptide–Membrane Complexes** *Rf* value of double-stranded peptides obtained using a mixed solvent such as CH_3OH–$CHCl_3$ (10%) on sililica gel plate according to the experimental section. The results were summarized in Table 3. The *Rf* value of **15a** (*Rf*=0.41) is larger than that of the diastereomers, **15b** (*Rf*=0.16) and **15c** (*Rf*=0.16). The *Rf* value of **17a** (*Rf*=0.42) and **18a** (*Rf*=0.52) is also larger than that of the **17b** (*Rf*=0.21) and **15b** (*Rf*=0.16), respectively, as shown in Table 3. The *Rf* values are a close relation to the polarity of the organic compounds, and the compounds of small *Rf* value have a high polarity. The *Rf* values are equivalent to the electric dipole moment as summarized in Table 1.

From the results, the *Rf* values of double-stranded peptides are related to the chirality. The *Rf* values of diastereomers such as (D-, L-) and (L-, D-) differ from that of the isomers, (L-, L-) and (D-, D-).

Figure 7 shows a 2-D plot using *Rf* values as the abscissa and Log(IC_{50}) as the ordinate. It suggests that the inhibitory effects of bis(y-Phe–x-Phe)$_2$–spacer(S) are related to the *Rf* value and D-form, that is, stereochemistry, while bis(y-

Phe–x-Phe)$_2$–spacer(S) possessed a high polarity and D-form has a function to outflow Ca^{2+} from the inner cell to the outer cell from the results of the previous section. If the double-stranded peptides have high polarity, hydrophobic property, and D-amino acid residue, the compounds are able to expect a powerful inhibitory effect against the tumor cells. Although we have no data as to whether bis(y-Phe–x-Phe)$_2$–spacer(S) affects the activity of the membrane calcium channels of A431 cell, the compounds may form the double-stranded peptide–membrane complexes, pores, or channel-like complexes by interaction with the cell membrane. Indeed, we have reported that the double-stranded peptide fluorescence probe conjugated dansyl group uptakes in the cell membrane.[2] By fluorometry using Fura2-AM, cytosolic $[Ca^{2+}]_c$ changes in the cells treated with the (L-, L-) and (D-, L-) forms of bis(y-Phe–x-Phe)$_2$–spacer(S).

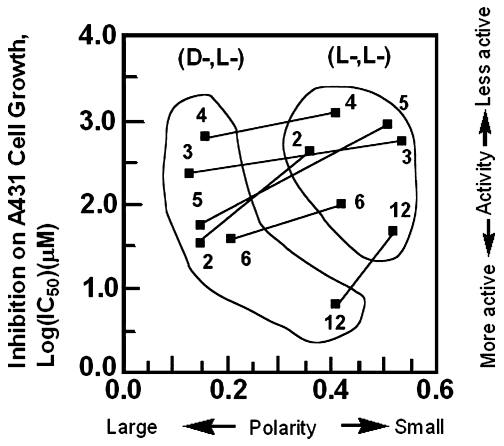

Fig. 7. Correlation between Polarity and IC_{50} against A431 Cells Growth Inhibition of Double-Stranded Peptides **13a**, **b**—**18a**, **b**

The number in the circle shows the number of carbons in spacer. All solid lines that have the connected square symbol become a left fall, and it shows that the (D-, L-) form have high inhibition for the cell proliferation.

The results for the changes in $[Ca^{2+}]_c$ show that (L-, L-) form of **18a** increases cytosolic Ca^{2+} concentration, however, (D-, L-), (L-, D-), and (D-, D-) forms of **18b**, **18c**, and **18d** containing D-Phe decrease cytosolic Ca^{2+} concentration against control A431 cells. We represent a proposed model of bis(y-Phe–x-Phe)$_2$spacer(S)–membrane complex as shown in Fig. 8. High polar (D-, L-), (L-, D-), and (D-, D-) forms **18b**, **18c**, and **18d** containing D-Phe turn out a large hole in the inner cell membrane. However, low polar (L-, L-) form **18a** no containing D-Phe may make a large hole in the outer cell membrane. The formation of a double-stranded peptide–membrane complex on the cell membrane may explain the reason for the increase or decrease of cytosolic Ca^{2+} concentration in the cells.

Conclusion

These studies showed the correlation between (L-, L-), (D-, L-), and (L-, D-) configurations of y-Phe–x-Phe sequence conjugated in double-stranded peptides and their properties on A549, A431, and *src*^{ts}NRK cells growth. The diasteremeric

Table 3. Relationship between Configuration and Polarity of Double-Stranded Peptides on A431 Cell Proliferation

Compound	Carbon number (n)	Configuration (y-, x-)	Polarity[a] (Rf)	IC_{50}[b] (μM)	$\log(IC_{50})$[c] (μM)
13a	2	(L-, L-)	0.36	426±2.50[b]	2.63
13b	2	(D-, L-)	0.15	34.3±0.800[b]	1.54
14a	3	(L-, L-)	0.53	574.0±6.50[b]	2.76
14b	3	(D-, L-)	0.13	237.0±4.50[b]	2.37
15a	4	(L-, L-)	0.41	1230.0>	3.09>
15b	4	(D-, L-)	0.16	639.0	2.81
16a	5	(L-, L-)	0.51	904.0	2.96
16b	5	(D-, L-)	0.15	56.5	1.75
17a	6	(L-, L-)	0.42	101.0	2.00
17b	6	(D-, L-)	0.21	39.1	1.59
18a	12	(L-, L-)	0.52	49.5±1.55[b]	1.69
18b	12	(D-, L-)	0.41	6.6	0.82

a) Polarity represents the mean of two *Rf* values at <±5% of the absolute error. *b*) IC_{50} values represent the mean±S.E.M. of the three independent determinations. The others represent the mean of two determinations at <±5% of the absolute error. *c*) Logarithm of IC_{50} value to the base 10. Each values are the log(mean).

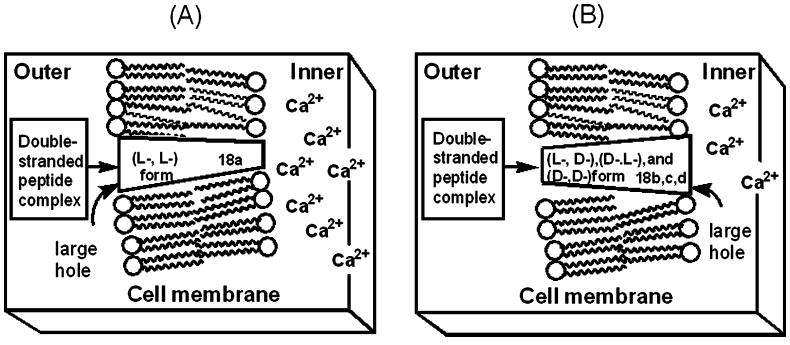

Fig. 8. Diasteromeric Effects of Changes in Cytosolic $[Ca^{2+}]_c$ and Proposed Model of Double-Stranded Peptide–Membrane Complexes

(A) Double-stranded peptide–membrane complexes are shown as a boxy in the cell membrane image. Cytosolic $[Ca^{2+}]$ concentration in A431 cells increases by treatment of compound **18a** contained the (L-, L-) form. (B) However, the concentration decreased after treatment of compounds **18b**, **c**, and **d** contained D-Phe.

chirality such as (D-, L-) and (L-, D-) configurations plays an important role in the inhibition of the growth of A431 and *src*^{ts}NRK cells. What is the role of growth inhibition of the D-Phe residue in the double-stranded peptide? One of the explanations is that the diastereomers, **18b** and **18c**, have stronger polarity than the enantiomers, **18a** and **18d**. When the double-stranded peptide uptake in the cell membrane, if it thinks that double-stranded peptide channels are formed in the channel (or pore), the changes of [Ca^{2+}] and permeability of Ca^{2+} may understand well.

Here, the results of the changes in [Ca^{2+}] indicate that although **18a** makes the large hole in the outer cell membrane, **18b**, **18c**, and **18d** form a large hole in the inner cell membrane. Stereo chemical control by bis(y-Phe–x-Phe)(S) on the cell growth or viability may provide new insights into the development and mechanism of anti-neoplastic reagents.

Acknowledgments We thank Dr. Hideki Suzuki, Tamiko Kiyotani, and Youichi Takase (Showa Pharmaceutical University, Tokyo) for NMR and FAB-MS measurements. We are grateful to Dr. Mitune Yamaguchi and Prof. Hiroshi Hojo (Showa Pharmaceutical University, Tokyo) for their help in the usage of the RF5000 fluorospectrophotometer.

References and Notes

1) Kobayashi S., Kobayashi H., Yamaguchi T., Nishida M., Yamaguchi K., Kurihara M., Miyata N., Tanaka A., *Chem. Pharm. Bull.*, **48**, 920—934 (2000).
2) Kobayashi S., Atuchi N., Kobayashi H., Shiraishi A., Hamashima H., Tanaka A., *Chem. Pharm. Bull.*, **52**, 204—213 (2004).
3) Misrahi M., Atger M., d'Auriol L., Loosfelt H., Merierl C., Fridiansky F., Guiochon-Mantel A., Galibert F., Milgrom E., *Biochem. Biophys. Res. Commun.*, **143**, 740—748 (1987).
4) Flood J. F., Roberts E., Sherman M. A., Kaplan B. E., Morley J. E., *Proc. Natl. Acad. Sci. U.S.A.*, **91**, 380—384 (1994).
5) Sticht H., Bayer P., Willbold D., Dammes S., Hilbich C., Beyreuther K., Frank R. W., Rosch P., *Eur. J. Biochem.*, **233**, 293—298 (1995).
6) Suzukake-Tsuchiya K., Moriya Y., Kawai H., Hori M., Uehara Y., Iinuma H., Naganawa H., Takeuchi T., *J. Antibiot.*, **44**, 344—348 (1991).
7) Uehara Y., Hori M., Takeuchi T., Umezawa H., *Jpn. J. Cancer Res.*,**76**, 672—675 (1985).
8) Nakagami Y., Minowa T., Tozuka K., Hiraoka Y., Nakajima H., Ishizaki I., Mastsumoto K., *Gan To Kagaku Ryoho*, **10**, 1993—1999 (1983).
9) Soule H. D., Vazquez J., Long A., Albert S., Brennan M. *J. Natl. Cancer Inst.*, **51**, 1409—1416 (1973).
10) Seiler N., Delcros J.-G., Moulinoux J.-P., *Int. J. Biochem. Cell. Biol.*, **28**, 843—861 (1996).
11) Grynkiewicz G., Poenie M., Tsien R. Y., *J. Biol. Chem.*, **260**, 3440—3450 (1985).
12) Spartan 04 and Spartan version 5.1 (Wavefunction, Inc., Irvine, CA), a molecular orbital software package. We calculated on the Pentium 4 (Windows) and Compaq AlphaStation DS10 (Tru64 Unix) machine, respectively.
13) DOJINDO LABORATORIES, Protocol P-14.
14) Grynkiewicz G., Poenie M., Tsien R. Y., *J. Biol. Chem.*, **260**, 3440—3450 (1985).
15) Wuthrich K., "NMR of Proteins and Nucleic Acids," John Wiley & Sons, Inc., New York, 1986.
16) Raghothama S., Chaddha M., Balaram P., *J. Phys. Chem.*, **100**, 19666—19671 (1996).
17) Delepierre M., Dobson C. M., Poulsen F. M., *Biochemistry*, **21**, 4756—4761 (1982).
18) Das C., Raghothama S., Balaram P., *J. Am. Chem. Soc.*, **120**, 5812—5813 (1998).
19) Cohen S. S., "A Guide to the Polyamines," Oxford University Press, New York, 1998.
20) Moulinoux J.-Ph., Quemener V., Khan N. A., *Cell. Mol. Biol.*, **37**, 773—783 (1991).